A Multireflect-Thru Method of Vector Network Analyzer Calibration

Arkadiusz Lewandowski, *Member, IEEE*, Wojciech Wiatr, *Member, IEEE*, Dazhen Gu, *Senior Member, IEEE*, Nathan D. Orloff, and James Booth

***Abstract*— We present a new method for two-port vector network analyzer (VNA) calibration, which uses multiple offset-reflect standards and a flush thru connection. Offset-reflect standards consist of sections of the same uniform transmission line with different lengths, which are terminated with the same highly reflective load. The unknown propagation constant of the transmission line and the load reflection coefficient are then determined simultaneously with the VNA calibration coefficients. We compare our method with the multiline thru-reflect-line (TRL) method and show that both methods yield similar results. Our new multireflect-thru method is solely based upon dimensional parameters of the calibration standards. Therefore, like the multiline TRL method, it can be used to establish a traceable VNA calibration. Thus, the multireflect-thru method constitutes an alternative to the multiline TRL calibration in environments in which the use of transmission lines is troublesome, such as in the case of VNAs with very small coaxial and waveguide connectors. The multireflect-thru method is also useful in on-wafer measurements since it allows us to keep a constant distance between the probes, which reduces the impact of crosstalk and speeds up automated testing.**

***Index Terms*— Calibration, error analysis, offset reflects, redundancy, vector network analyzer (VNA).**

I. Introduction

WE PRESENT a novel method of two-port vector network analyzer (VNA) calibration, which uses multiple offset-reflect standards and a thru standard. Offset-reflect standards consist of uniform transmission-line sections with different lengths terminated with the same highly reflective load, typically a short or an open circuit, while the thru is realized as a direct connection of VNA ports (flush thru).

The problem of calibrating a VNA with such standards has long been present in the literature [1]–[9]. References [1], [6] present a one-port VNA calibration method which realizes offset reflects with a sliding short. The sliding short is assumed to be lossless, and its positions need not to be known. A circle is then fitted to the sliding short measurements whose center and radius are related to calibration coefficients. Based on the circle parameters and measurements of two other additional standards (one of them can also be a sliding load [1]), calibration is completed. Methods [1], [6] are, however, limited to lossless offset shorts.

References [3]–[5] present a different implementation of a one-port VNA calibration method that accounts for losses in the sliding-short transmission line. This method requires neither the sliding-short losses nor its positions to be known. However, a measurement of an ideal matched termination [3] or a sliding load [4], [5] is needed. Therefore, these methods are inconvenient at higher frequencies where fixed terminations with low reflections are unavailable, while the realization of a sliding load is either difficult (e.g., for coaxial connectors with small diameter) or impossible (e.g., on-wafer environments).

Reference [7] extends the method of [3]–[5], and calibrates a one-port VNA solely based on measurements of offset-reflect standards. This method employs a model for frequency dependence of offset-line phase-constant in order to estimate the unknown lengths of the offset lines and their attenuation constant. The resulting problem is solved iteratively with a nonlinear least squares optimization. This method is further extended in [9] to the problem of two-port VNA calibration by assuming that the offset reflects are terminated with an unknown load whose reflection coefficient is determined from the thru measurement. The drawback of methods [7], [9] is the requirement for the model of the phase constant which might be difficult to obtain for transmission lines with large losses or high dispersion. Also, these methods may not yield a unique solution due to the use of optimization techniques that suffer from the local-minima problem.

Reference [8] presents another method that requires the attenuation constant of the offset shorts and the termination reflection-coefficient to be known, while the phase shift of the offset-short reflection coefficients is determined during the calibration. The resulting problem is also solved iteratively with a nonlinear least squares optimization. The drawback of this approach is that it requires precise measurements of conductor surface followed by electromagnetic simulations in order to obtain the transmission-line attenuation constant and the short-circuit impedance. Also, this method, similar to [7], may not give a unique solution due to the use of optimization techniques.

In this paper, we introduce a new method for calibrating a two-port VNA with multiple offset-reflects and a flush thru connection, which determines the unknown propagation

Manuscript received April 7, 2016; revised August 17, 2016 and October 17, 2016; accepted October 25, 2016. Date of publication December 29, 2016; date of current version March 3, 2017. This work was supported by the Polish National Science Center under Project 2011/03/D/ST7/01731.

A. Lewandowski and W. Wiatr are with the Institute of Electronic Systems, Warsaw University of Technology, 00-665 Warsaw, Poland (e-mail: a.lewandowski@elka.pw.edu.pl; w.wiatr@elka.pw.edu.pl).

D. Gu, N. D. Orloff, and J. Booth are with the National Institute of Standards and Technology, Boulder, CO 80305 USA (e-mail: dazhen.gu@nist.gov; nathan.orloff@nist.gov).

Color versions of one or more of the figures in this paper are available online at http://ieeexplore.ieee.org.

Digital Object Identifier 10.1109/TMTT.2016.2627036

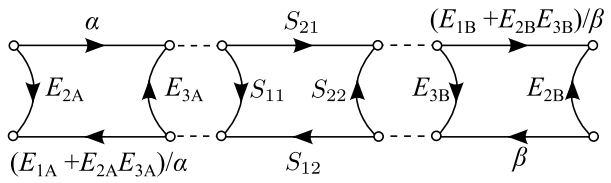

Fig. 1. Two-port VNA measurement model used in the multireflect-thru calibration method.

constant of the offset reflects and the terminating-impedance reflection coefficient based only on the knowledge of the offset-reflect lengths and without the use of troublesome optimization techniques. The VNA calibration coefficients and reflection coefficient of the termination impedance are calculated from closed-form expressions, while the propagation constant is determined by solving $N-3$ independent complex-valued nonlinear equations, where N is the number of offset-reflect standards. As a starting point for these equations, we need only an approximate estimate of the propagation constant which can be easily obtained based on the dimensional and material parameters of the transmission-line sections in the offset reflects.

The principle of our method is very similar to that of the multiline thru-reflect-line (TRL) calibration [10], and is based on averaging solutions of basic nonredundant calibrations that are constructed from measurements of four different offset reflects on each VNA port. These measurements, supplemented with a flush thru measurement, form the thru-reflect-reflect-reflect-reflect (T4R) calibration, which we present in Section II. In the following sections, we discuss the averaging technique (see Section III), and then present an experimental verification of our method (see Section IV), in which we compare corrected measurements of a verification device performed after calibrating a VNA with our new multireflect-thru method and with the multiline TRL technique. Finally, in Section V, we draw some conclusions.

II. Thru-Reflect-Reflect-Reflect-Reflect Calibration

In this section, we present the theory of the T4R calibration method. We start off with an overview of the VNA model and the calibration scheme. Then, we discuss calibration of a single VNA reflectometer with four different offset-reflect standards. Finally, we show how to complete the two-port VNA calibration by use of a flush thru measurement.

A. VNA Model

A model for two-port VNA measurement we use is shown in Fig. 1. This model is based on the error-box model of [11], however, it uses an alternative set of parameters. We assume that the switch terms have been measured separately and corrected for by the use of approach [11]. We also assume that the isolation terms are negligible. Based on that, for a two-port device under test (DUT) with the scattering matrix $\mathbf{S}$ and the corresponding transmission matrix $\mathbf{T}$ given by

$$\mathbf{S}=\begin{bmatrix} S_{11} & S_{12} \\ S_{21} & S_{22} \end{bmatrix} \quad \mathbf{T}=\frac{1}{S_{21}}\begin{bmatrix} -\det\mathbf{S} & S_{11} \\ -S_{22} & 1 \end{bmatrix} \tag{1}$$

we have the corresponding measured (raw) scattering $\widetilde{\mathbf{S}}$ and transmission $\widetilde{\mathbf{T}}$ matrices where the tilde "$\sim$" on top of the symbol denotes the measurement.

Now, matrix $\widetilde{\mathbf{T}}$ is the transmission matrix of the network shown in Fig. 1, that is,

$$\widetilde{\mathbf{T}}=\frac{1}{E_t}\mathbf{E}_A\mathbf{T}\mathbf{E}_B \tag{2}$$

where

$$\mathbf{E}_A=\begin{bmatrix} E_{1A} & E_{2A} \\ -E_{3A} & 1 \end{bmatrix} \quad \mathbf{E}_B=\begin{bmatrix} E_{1B} & E_{3B} \\ -E_{2B} & 1 \end{bmatrix} \tag{3}$$

and

$$E_t=\frac{\alpha}{\beta}(E_{1B}+E_{2B}E_{3B}). \tag{4}$$

Thus, the VNA model parameters are E_{1A}, E_{2A}, and E_{3A} (which describe the left VNA reflectometer), E_{1B}, E_{2B}, and E_{3B} (which describe the right VNA reflectometer), and the parameter E_t.

B. Calibration Scheme

In the T4R calibration scheme, one measures four offset-reflect standards on each VNA port, and a flush thru connection of these ports. Offset-reflect standards consist of uniform transmission-line sections terminated with a highly reflective load. The transmission-line sections of the offset reflects used on VNA ports A and B have lengths l_{Ai} and l_{Bi}, for $i=0,\ldots,3$, and propagation constants γ_A and γ_B, respectively. The terminating load has the same reflection coefficient Γ_T for all of the offset reflects.[1] Thus, the nominal reflection coefficient of the offset-reflect standards can be written as[2]

$$\Gamma_{Ai}=\Gamma_T e^{-2\gamma_A l_{Ai}}, \quad \Gamma_{Bi}=\Gamma_T e^{-2\gamma_B l_{Bi}} \tag{5}$$

while their raw measurements are denoted by $\widetilde{\Gamma}_{Ai}$ and $\widetilde{\Gamma}_{Bi}$.

Based on the flow graph in Fig. 1, we can write the relationship between raw measurements and definitions the of the offset reflects as

$$\widetilde{\Gamma}_{Ai}=\frac{E_{2A}+E_{1A}\Gamma_{Ai}}{1-E_{3A}\Gamma_{Ai}} \quad \widetilde{\Gamma}_{Bi}=\frac{E_{2B}+E_{1B}\Gamma_{Bi}}{1-E_{3B}\Gamma_{Bi}} \tag{6}$$

for $i=0,\ldots,3$. We can further lump the unknown reflection coefficient Γ_T into the reflectometer parameters by rewriting (6) with normalized calibration coefficients

$$E'_{1A}=E_{1A}\Gamma_T \quad E'_{3A}=E_{3A}\Gamma_T \tag{7}$$

$$E'_{1B}=E_{1B}\Gamma_T \quad E'_{3B}=E_{3B}\Gamma_T \tag{8}$$

and with normalized reflection-coefficient of the offset reflects

$$\rho_{Ai}=\frac{\Gamma_{Ai}}{\Gamma_T}=e^{-2\gamma_A l_{Ai}} \quad \rho_{Bi}=\frac{\Gamma_{Bi}}{\Gamma_T}=e^{-2\gamma_B l_{Bi}} \tag{9}$$

[1]We assume that the characteristic impedance for offset sections on ports A and B is the same, thus for the same terminating impedance Z_T, we have $\Gamma_{TA}=\Gamma_{TB}=\Gamma_T$. In a general case, when these impedances are different, we have $\Gamma_{TA}\neq\Gamma_{TB}$. This case will not be considered here.

[2]Similar to the multiline TRL method [10], we assume that connection interface is the *same* for all calibration standards and DUTs, and thus gets lumped into the VNA calibration coefficients. Therefore, we do not include its description in the definition of the calibration standards. This assumption is very well met for typical on-wafer, coaxial, and rectangular-waveguide measurement situations. However, it may be violated for smaller coaxial and waveguide connectors. This last case will not be discussed here.

that yields

$$\widetilde{\Gamma}_{Ai} = \frac{E_{2A} + E'_{1A}\rho_{Ai}}{1 - E'_{3A}\rho_{Ai}} \quad \widetilde{\Gamma}_{Bi} = \frac{E_{2B} + E'_{1B}\rho_{Bi}}{1 - E'_{3B}\rho_{Bi}}. \tag{10}$$

We will further on refer to the reflectometers described by the parameters E'_{1A}, E_{2A}, E'_{3A}, and E'_{1B}, E_{2B}, E'_{3B} as reduced reflectometers.

The thru standard is realized as a direct connection of the VNA ports (flush thru), thus its transmission matrix $\mathbf{T}_t$ is the identity matrix. The raw measurement of the thru standard is thus given by

$$\widetilde{\mathbf{T}}_t = \frac{1}{E_t}\mathbf{E}_A\mathbf{E}_B \tag{11}$$

which can be written with the normalized calibration coefficients (7) and (8) as [9]

$$\widetilde{\mathbf{T}}_t = \frac{1}{E_t}\mathbf{E}'_A\mathbf{\Gamma}\mathbf{\Gamma}\mathbf{E}'_B \tag{12}$$

where

$$\mathbf{E}'_A = \begin{bmatrix} E'_{1A} & E_{2A} \\ -E'_{3A} & 1 \end{bmatrix} \quad \mathbf{E}'_B = \begin{bmatrix} E'_{1B} & E'_{3B} \\ -E_{2B} & 1 \end{bmatrix} \tag{13}$$

are the reduced-reflectometers parameters and

$$\mathbf{\Gamma} = \begin{bmatrix} \Gamma_T^{-1} & 0 \\ 0 & 1 \end{bmatrix}. \tag{14}$$

In the following, we describe the solution of the set of nonlinear equations (10) and (12). We first determine the unknown propagation constants γ_A and γ_B, and parameters of the reduced reflectometers. Then, we determine the remaining terms Γ_T and E_t from the thru measurement.

C. Reduced-Reflectometer Calibration

The calibration equations (10) for both reflectometers are independent of each other and have identical form, thus they are solved in the same manner. Therefore, in the following, we will omit the symbols A and B in subscripts.

The set (10) consists of four equations for four unknown parameters: E'_1, E_2, E'_3, and γ, where the dependence on γ is given by (9). We may rewrite (10) as

$$\underbrace{\begin{bmatrix} \rho_0 & 1 & \rho_0\widetilde{\Gamma}_0 & -\widetilde{\Gamma}_0 \\ \rho_1 & 1 & \rho_1\widetilde{\Gamma}_1 & -\widetilde{\Gamma}_1 \\ \rho_2 & 1 & \rho_2\widetilde{\Gamma}_2 & -\widetilde{\Gamma}_2 \\ \rho_3 & 1 & \rho_3\widetilde{\Gamma}_3 & -\widetilde{\Gamma}_3 \end{bmatrix}}_{\mathbf{P}(\gamma)} \underbrace{\begin{bmatrix} E'_1 \\ E_2 \\ E'_3 \\ 1 \end{bmatrix}}_{\mathbf{x}} = 0. \tag{15}$$

Since the norm $||\mathbf{x}||$ of the vector $\mathbf{x}$ is by definition different from zero, the homogeneous set of equations (15) is fulfilled only if

$$\det \mathbf{P}(\gamma) = 0 \tag{16}$$

which yields a nonlinear equation for γ. This equation is solved numerically by the use of a modified Newton–Raphson method [12]. Details of this method are given in Appendix A.

Having solved for γ, we can remove one of the equations in (15), plug the value of γ into (9) and solve the resulting set of linear equations. Removing, for example, the first equation, we obtain

$$\begin{bmatrix} E'_1 \\ E_2 \\ E'_3 \end{bmatrix} = \begin{bmatrix} \rho_1 & 1 & \rho_1\widetilde{\Gamma}_1 \\ \rho_2 & 1 & \rho_2\widetilde{\Gamma}_2 \\ \rho_3 & 1 & \rho_3\widetilde{\Gamma}_3 \end{bmatrix}^{-1} \begin{bmatrix} \widetilde{\Gamma}_1 \\ \widetilde{\Gamma}_2 \\ \widetilde{\Gamma}_3 \end{bmatrix} \tag{17}$$

which completes the reduced-reflectometer calibration.

D. Determining Γ_T and E_t

In the next step, we use the solutions of the reduced-reflectometer calibration given by (16) and (17), and the thru measurement (12) to determine Γ_T and E_t. We first write out the diagonal terms of the matrix $\widetilde{\mathbf{T}}_t$

$$\widetilde{T}_{11t} = \frac{E'_{1A}E'_{1B} - E_{2A}E_{2B}\Gamma_T^2}{E_t\Gamma_T^2} \quad \widetilde{T}_{22t} = \frac{\Gamma_T^2 - E'_{3A}E'_{3B}}{E_t\Gamma_T^2}. \tag{18}$$

Now, from the ratio of these terms $\widetilde{T}_{11t}/\widetilde{T}_{22t} = -\det\widetilde{\mathbf{S}}_t$, where $\widetilde{\mathbf{S}}_t$ is the measured (raw) scattering matrix of the thru, we obtain the following equation:

$$\Gamma_T = \pm\sqrt{\frac{E'_{1A}E'_{1B} - \det\widetilde{\mathbf{S}}_t E'_{3A}E'_{3B}}{E_{2A}E_{2B} - \det\widetilde{\mathbf{S}}_t}}. \tag{19}$$

Similar to the classical TRL algorithm [13], [14], in order to pick the root of (19), we use an estimate of Γ_T phase.

In order to obtain E_t, we first denormalize the calibration coefficients E'_{1A}, E'_{3A}, and E'_{1B}, E'_{3B} based on the definitions (7) and (8), and Γ_T obtained from (19). We then take the determinant of (11), which leads to the following equation:

$$\det\widetilde{\mathbf{T}}_t = \frac{\widetilde{S}_{12t}}{\widetilde{S}_{21t}} = \frac{\det\mathbf{E}_A\det\mathbf{E}_B}{E_t^2} \tag{20}$$

thus

$$E_t = \pm\sqrt{\frac{\widetilde{S}_{21t}}{\widetilde{S}_{12t}}\det\mathbf{E}_A\det\mathbf{E}_B}. \tag{21}$$

The sign of E_t is chosen by inserting (21) into the prediction (11) of the thru transmission matrix, and verifying for which solution of (21), the norm (e.g., the Frobenius matrix norm [15]) of the difference between this prediction and the actual raw transmission matrix of the thru is smaller.

III. Calibration With a Redundant Number of Reflect Standards

In this section, we present a technique for performing a two-port VNA calibration with more than four reflect standards. This technique builds on the basic T4R calibration method described in Section II.

A. Overview

When calibrating a two-port VNA with more than four reflect standards, we proceed in a similar manner as in the case of the T4R calibration. We first determine the normalized calibration coefficients of both VNA reflectometers, and then complete the calibration by determining the parameters Γ_T and E_t.

In order to determine the normalized calibration coefficients, we average results of multiple reduced-reflectometer calibrations constructed from different four-element subsets of the entire set of N offset-reflect standards. Although there are $C_4^N = N!/(N-4)!4!$ such subsets, we can construct only $K = N-3$ subsets that introduce new information. Indeed, when using four reflect standards, we obtain a single solution of the reduced-reflectometer calibration defined by (15). Thus, by adding each offset-reflect standard, we add only one degree of freedom, consequently we can only obtain $N-3$ independent reduced-reflectometer calibrations.

Assuming that the reflect standards are numbered from 0 to $N-1$, the kth subset is uniquely defined by a four-element vector of ordered reflect-standard indices

$$\mathbf{i}_k = [i_{k_0}, i_{k_1}, i_{k_2}, i_{k_3}]^T \tag{22}$$

where $0 \le i_{k_0} < i_{k_1} < i_{k_2} < i_{k_3} < N$, and $k = 0, \ldots, K-1$. We refer to a particular set of four-element subsets of the reflect standards, which is defined by the vectors $\mathbf{i}_k$ for $k = 0, \ldots, K-1$, as an *averaging scheme*.

We perform the reduced-reflectometer calibration described in Section II-C for each of the K subsets. As a result, for the kth subset, we obtain the solution

$$\boldsymbol{\beta}_k = \left[E'_{1k}, E_{2k}, E'_{3k}, \gamma_k\right]^T. \tag{23}$$

The errors in reflection coefficients of offset reflects used in the kth subset[3]

$$\Delta\mathbf{y}_k = \left[\frac{\Delta\rho_{i_{k_0}}}{\rho_{i_{k_0}}}, \frac{\Delta\rho_{i_{k_1}}}{\rho_{i_{k_1}}}, \frac{\Delta\rho_{i_{k_2}}}{\rho_{i_{k_2}}}, \frac{\Delta\rho_{i_{k_3}}}{\rho_{i_{k_3}}}\right]^T$$

cause an error in the solution

$$\Delta\boldsymbol{\beta}_k = \left[\Delta E'_{1k}, \Delta E_{2k}, \Delta E'_{3k}, \Delta\gamma_k\right]^T \tag{24}$$

which based on (B.6) can be written as

$$\mathbf{X}_k \Delta\boldsymbol{\beta}_k = -\Delta\mathbf{y}_k \tag{25}$$

where

$$\mathbf{X}_k = \mathbf{X}_{0,k}\mathbf{E}_k \tag{26}$$

$$\mathbf{X}_{0,k} = \begin{bmatrix} \rho_{i_{k_0}} & 1 & \rho_{i_{k_0}}^{-1} & -2l_{i_{k_0}} \\ \rho_{i_{k_1}} & 1 & \rho_{i_{k_1}}^{-1} & -2l_{i_{k_1}} \\ \rho_{i_{k_2}} & 1 & \rho_{i_{k_2}}^{-1} & -2l_{i_{k_2}} \\ \rho_{i_{k_3}} & 1 & \rho_{i_{k_3}}^{-1} & -2l_{i_{k_3}} \end{bmatrix} \tag{27}$$

and

$$\mathbf{E}_k = \begin{bmatrix} -E'_{3k} & 0 & E'_{1k} & 0 \\ 1 & -E'_{3k} & E_{2k} & 0 \\ 0 & 1 & 0 & 0 \\ 0 & 0 & 0 & E'_{1k} + E_{2k}E'_{3k} \end{bmatrix}. \tag{28}$$

We see that each solution $\boldsymbol{\beta}_k$ has in general different errors which depend on the choice of the reflect standards in the kth subset and relative errors $\Delta\mathbf{y}_k$ in their reflection coefficients. Therefore, in order to determine the estimate of normalized calibration coefficient of a VNA reflectometer, we determine a weighted average of these solutions.

[3]We decided to express these errors in a relative-error form due to a convenient interpretation for the practical case of offset reflects with low losses (i.e., when $|\Gamma| \approx 1$): the real and imaginary parts of the relative error $\Delta\rho/\rho$ are then the in-phase and quadrature error component, respectively (see [16]). Indeed, $\Delta\Gamma^{IQ} = \Delta\Gamma|\Gamma|/\Gamma \approx \Gamma_T\Delta\rho/(\Gamma_T\rho) = \Delta\rho/\rho$.

B. Averaging Results of Reduced-Reflectometer Calibrations

The statistical model for the solutions $\boldsymbol{\beta}_k$ can be written in a compact form as an overdetermined set of equations

$$\mathbf{I}\boldsymbol{\beta} = \underline{\boldsymbol{\beta}} + \underline{\Delta\boldsymbol{\beta}} \tag{29}$$

where the vector $\underline{\boldsymbol{\beta}}$ is comprised of solutions from individual reduced-reflectometer calibrations and the vector $\underline{\Delta\boldsymbol{\beta}}$ contains errors in those solutions. Both vectors have size $\overline{4K} \times 1$ and are given by

$$\underline{\boldsymbol{\beta}} = \begin{bmatrix} \boldsymbol{\beta}_0 \\ \vdots \\ \boldsymbol{\beta}_{K-1} \end{bmatrix}, \quad \underline{\Delta\boldsymbol{\beta}} = \begin{bmatrix} \Delta\boldsymbol{\beta}_0 \\ \vdots \\ \Delta\boldsymbol{\beta}_{K-1} \end{bmatrix} \tag{30}$$

while the matrix $\mathbf{I}$ has size $4K \times 4$ and is given by

$$\mathbf{I} = \begin{bmatrix} \mathbf{I}_4 \\ \vdots \\ \mathbf{I}_4 \end{bmatrix} \tag{31}$$

and $\mathbf{I}_4$ is a 4×4 identity matrix.

The relationship (29) could be directly used to determine the estimate $\boldsymbol{\beta}$ based on the covariance matrix of $\underline{\Delta\boldsymbol{\beta}}$. However, it is more convenient to transform it to a form, in which the error vectors $\Delta\mathbf{y}_k$ are given explicitly. To this end, we first rewrite the relationship (25) between the error vectors $\Delta\boldsymbol{\beta}_k$ and $\Delta\mathbf{y}_k$, for $k = 0, \ldots, K-1$, in a more compact form

$$\underline{\mathbf{X}}\,\underline{\Delta\boldsymbol{\beta}} = -\underline{\Delta\mathbf{y}} \tag{32}$$

where the matrix $\underline{\mathbf{X}}$ and vector $\underline{\Delta\mathbf{y}}$ have size $4K \times 4K$ and $4K \times 1$, respectively, and are given by

$$\underline{\mathbf{X}} = \begin{bmatrix} \mathbf{X}_0 & & \\ & \ddots & \\ & & \mathbf{X}_{K-1} \end{bmatrix}, \quad \underline{\Delta\mathbf{y}} = \begin{bmatrix} \Delta\mathbf{y}_0 \\ \vdots \\ \Delta\mathbf{y}_{K-1} \end{bmatrix}. \tag{33}$$

We then premultiply (29) by $\underline{\mathbf{X}}$, which after inserting (32) yields

$$\underline{\mathbf{Y}}\boldsymbol{\beta} = \underline{\mathbf{X}}\,\underline{\boldsymbol{\beta}} - \underline{\Delta\mathbf{y}}. \tag{34}$$

with

$$\underline{\mathbf{Y}} = \underline{\mathbf{X}}\mathbf{I} = \begin{bmatrix} \mathbf{X}_0 \\ \vdots \\ \mathbf{X}_{K-1} \end{bmatrix}. \tag{35}$$

In order to solve the overdetermined set of equations (34) for $\boldsymbol{\beta}$, we first note that the covariance matrix for the error vector $\underline{\Delta\mathbf{y}}$ is singular and cannot be inverted. Indeed, this matrix has size $4K \times 4K$, where $K = N-3$, while its rank is N. Thus, (34) cannot be solved by use of the traditional Gauss–Markov theorem [17]. Therefore, we need to use the modification [18] of the Gauss–Markov theorem for the case of a singular covariance matrix. To this end, we first construct the covariance matrix for the vector $\underline{\Delta\mathbf{y}}$. We can write

$$\underline{\Delta\mathbf{y}} = \mathbf{C}\mathbf{e} \tag{36}$$

where

$$\mathbf{e} = \left[\frac{\Delta\rho_0}{\rho_0}, \ldots, \frac{\Delta\rho_{N-1}}{\rho_{N-1}}\right]^T. \tag{37}$$

Matrix $\mathbf{C}$ has size $4K \times N$ and captures the averaging scheme (22): if the nth reflect standard is used in the kth subset at the position $i \in \{1, 2, 3, 4\}$, then the element $c_{4k+i,n}$ of the matrix $\mathbf{C}$ equals one, and otherwise zero. Since we cannot include the same reflect standard more than once in a single reduced-reflectometer calibration, columns of the matrix $\mathbf{C}$ are orthogonal.

With the use of this definition, the covariance matrix for $\underline{\Delta\mathbf{y}}$ is given as

$$\mathbf{\Sigma}_{\underline{\Delta\mathbf{y}}} = \mathbf{C}\mathbf{\Sigma}_{\mathbf{e}}\mathbf{C}^H \tag{38}$$

where the superscript "H" denotes the conjugate transpose, and $\mathbf{\Sigma}_{\mathbf{e}} = \mathrm{E}[\mathbf{e}\mathbf{e}^H]$ is the covariance matrix of relative errors $\mathbf{e}$ in offset-reflect reflection coefficients.[4] By use of the Gauss–Markov theorem for the case of singular covariance matrix [18], we can write the equation for averaged solution $\hat{\boldsymbol{\beta}}$ of reduced-reflectometer calibration as

$$\left(\underline{\mathbf{Y}}^H \mathbf{\Sigma}^+_{\underline{\Delta\mathbf{y}}} \underline{\mathbf{Y}}\right)\hat{\boldsymbol{\beta}} = \underline{\mathbf{Y}}^H \mathbf{\Sigma}^+_{\underline{\Delta\mathbf{y}}} \underline{\mathbf{X}}\,\underline{\boldsymbol{\beta}} \tag{39}$$

where the superscript $^+$ denotes the Moore–Penrose matrix pseudoinverse [21]. Accounting for the properties of this inverse, we can further write

$$\mathbf{\Sigma}^+_{\underline{\Delta\mathbf{y}}} = (\mathbf{C}^+)^H \mathbf{\Sigma}_{\mathbf{e}}^{-1} \mathbf{C}^+ \tag{40}$$

where $\mathbf{C}^+$ has size $N \times 4K$. We can easily show that if the nth reflect standard is used in the kth subset at the position $i \in \{1, 2, 3, 4\}$ then the element $c^+_{n,4k+i}$ of the matrix $\mathbf{C}^+$ will be equal to $1/N_n$ where N_n is the number of individual reduced-reflectometer calibrations that include the nth reflect, and otherwise zero.

Now, solving (39), we can finally write our main result, that is, the averaged estimate of reduced-reflectometer parameters

$$\hat{\boldsymbol{\beta}} = \mathbf{M}^{-1} \underline{\mathbf{Y}}^H \mathbf{\Sigma}^+_{\underline{\Delta\mathbf{y}}} \underline{\mathbf{X}}\,\underline{\boldsymbol{\beta}} \tag{41}$$

where

$$\mathbf{M} = \underline{\mathbf{Y}}^H \mathbf{\Sigma}^+_{\underline{\Delta\mathbf{y}}} \underline{\mathbf{Y}} = (\mathbf{C}^+\underline{\mathbf{Y}})^H \mathbf{\Sigma}_{\mathbf{e}} (\mathbf{C}^+\underline{\mathbf{Y}}) \tag{42}$$

is the Fisher matrix [17]. The covariance matrix of this solution may be further determined as

$$\begin{aligned}\mathbf{\Sigma}_{\hat{\boldsymbol{\beta}}} &= \mathrm{E}[\hat{\boldsymbol{\beta}}\hat{\boldsymbol{\beta}}^H] \\ &= \mathbf{M}^{-1} \underline{\mathbf{Y}}^H \mathbf{\Sigma}^+_{\underline{\Delta\mathbf{y}}} \mathbf{\Sigma}_{\underline{\mathbf{X}}\,\underline{\boldsymbol{\beta}}} \left(\mathbf{\Sigma}^+_{\underline{\Delta\mathbf{y}}}\right)^H \underline{\mathbf{Y}} \mathbf{M}^{-H}.\end{aligned} \tag{43}$$

Taking into account that $\mathbf{\Sigma}_{\underline{\mathbf{X}}\,\underline{\boldsymbol{\beta}}} = \mathbf{\Sigma}_{\underline{\Delta\mathbf{y}}}$, and $(\mathbf{\Sigma}^+_{\underline{\Delta\mathbf{y}}})^H = (\mathbf{\Sigma}^H_{\underline{\Delta\mathbf{y}}})^+ = \mathbf{\Sigma}^+_{\underline{\Delta\mathbf{y}}}$, and also accounting for the properties of the Moore–Penrose pseudoinverse ($\mathbf{A}^+\mathbf{A}\mathbf{A}^+ = \mathbf{A}^+$), we easily obtain

$$\mathbf{\Sigma}_{\hat{\boldsymbol{\beta}}} = \mathbf{M}^{-1}\mathbf{M}\mathbf{M}^{-H} = \mathbf{M}^{-1} \tag{44}$$

since the Fisher matrix is Hermitian.

[4]We make an approximation that the real and imaginary parts of each error $\Delta\rho/\rho$ have the same variance and are uncorrelated. This approximation allows us to use a much simpler complex-valued notation for the error propagation, however, at the cost of slightly larger variances of the calibration result (see [19]). Generalization to the case of an arbitrary normal distribution is straightforward, however, it involves a more complicated block-matrix-based notation (see [20]).

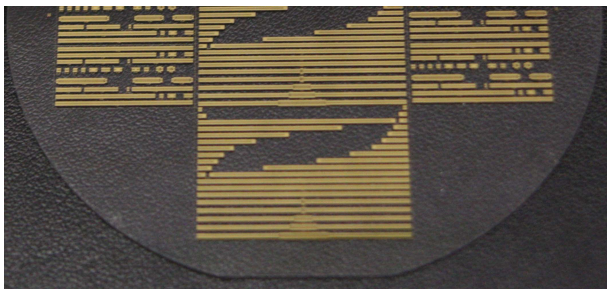

Fig. 2. Photograph of the quartz wafer with two multireflect-thru sets (middle-top and middle-bottom), and two multiline TRL sets (top-left and top-right).

C. Optimal Averaging Scheme

When developing the averaging technique in Section III-B, we assumed that the N offset reflects are in some manner divided into $K = N - 3$ four-element subsets; this division was referred to as the averaging scheme. Below, we discuss the choice of the averaging scheme that provides an accurate and robust calibration. Our discussion will be based on the analysis of how this scheme affects the covariance matrix (44).

We first note that, based on (26) and (35), we can write matrix $\underline{\mathbf{Y}}$ as

$$\underline{\mathbf{Y}} = \begin{bmatrix}\mathbf{X}_0 \\ \vdots \\ \mathbf{X}_{K-1}\end{bmatrix} = \begin{bmatrix}\mathbf{X}_{0,0}\mathbf{E}_0 \\ \vdots \\ \mathbf{X}_{0,K-1}\mathbf{E}_{K-1}\end{bmatrix}. \tag{45}$$

Now, if all of the basic calibrations are well-conditioned, all of the individual results $\boldsymbol{\beta}_k$ are close to the solution $\hat{\boldsymbol{\beta}}$ given by (41), thus $\mathbf{E}_k \approx \hat{\mathbf{E}}$, for $k = 0, \ldots, K-1$, where

$$\hat{\mathbf{E}} = \begin{bmatrix}-\hat{E}'_3 & 0 & \hat{E}'_1 & 0 \\ 1 & -\hat{E}'_3 & \hat{E}_2 & 0 \\ 0 & 1 & 0 & 0 \\ 0 & 0 & 0 & -\hat{E}'_1 + \hat{E}_2\hat{E}'_3\end{bmatrix}. \tag{46}$$

Consequently, we can approximate

$$\underline{\mathbf{Y}} \approx \begin{bmatrix}\mathbf{X}_{0,0} \\ \vdots \\ \mathbf{X}_{0,K-1}\end{bmatrix}\mathbf{E} = \underline{\mathbf{Y}_0}\hat{\mathbf{E}} \tag{47}$$

and therefore approximate the Fisher matrix as

$$\begin{aligned}\mathbf{M} &\approx (\mathbf{C}^+\underline{\mathbf{Y}_0}\hat{\mathbf{E}})^H \mathbf{\Sigma}_{\mathbf{e}} (\mathbf{C}^+\underline{\mathbf{Y}}\hat{\mathbf{E}}) \\ &= \hat{\mathbf{E}}^H (\mathbf{C}^+\underline{\mathbf{Y}_0})^H \mathbf{\Sigma}_{\mathbf{e}} (\mathbf{C}^+\underline{\mathbf{Y}_0})\hat{\mathbf{E}}.\end{aligned} \tag{48}$$

Now, we can show that the approximate Fisher matrix (48), and consequently the resulting covariance matrix given by (44), do not depend on the particular choice of the averaging scheme. Indeed, consider the product $\mathbf{C}^+\underline{\mathbf{Y}_0}$. Let N_n be the number of T4R calibrations that include the nth

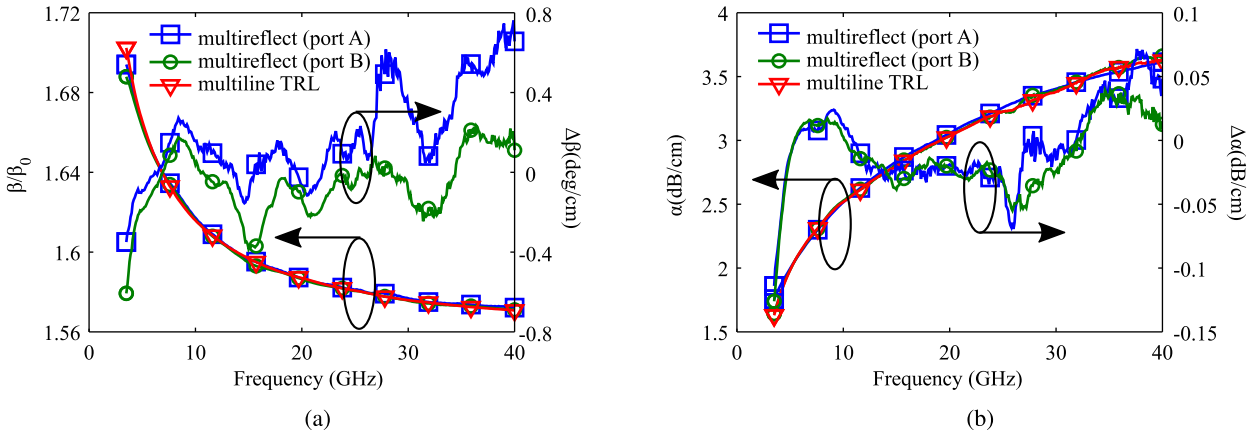

Fig. 3. Propagation constant obtained with the multireflect-thru calibration and from the reference multiline TRL method. (a) Phase constant β normalized to vacuum phase constant β_0 obtained from reduced-reflectometer calibrations on port A (blue solid line with squares) and port B (green solid line with circles), and from the multiline TRL (red solid line with triangles) along with differences with respect to the multiline TRL result. (b) Attenuation constant for both reduced reflectometer calibrations and differences with respect to the multiline TRL result (the same colors and markers as for the phase constant).

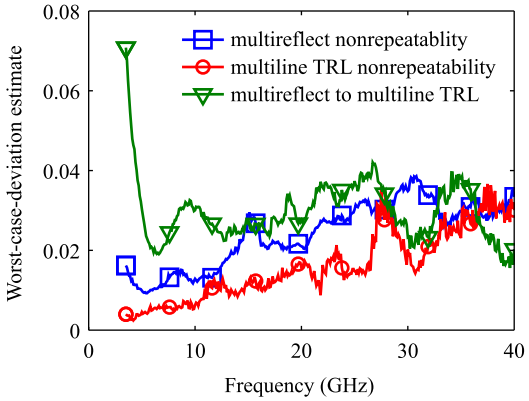

Fig. 4. Estimate of the worst case deviations in a measurement of a two-port device with $|S_{ij}| \leq 1$ due to nonrepeatability of the multireflect-thru calibration (blue solid line with squares), nonrepeatability of the reference multiline TRL calibration (red solid line with circles), and difference between both calibrations (green solid line with triangles).

reflect standard. The element $c^{+}_{n,4k+i}$ of the matrix $\mathbf{C}^{+}$ will be equal to $1/N_n$ if the nth reflect standard is used in the kth subset at the position $i \in \{1, 2, 3, 4\}$, and otherwise zeros. On the other hand, we see from (35) if the nth reflect standard is used in the kth subset at the position $i \in \{1, 2, 3, 4\}$, then the $(4k + i)$th row of $\underline{\mathbf{Y}_0}$ has the form $[\rho_n, 1, \rho_n^{-1}, -2l_n]$. Consequently, we can easily show that

$$\mathbf{C}^{+}\underline{\mathbf{Y}_0} = \begin{bmatrix} \rho_1 & 1 & \rho_1^{-1} & -2l_1 \\ \rho_2 & 1 & \rho_2^{-1} & -2l_2 \\ \vdots & \vdots & \vdots & \vdots \\ \rho_N & 1 & \rho_N^{-1} & -2l_N \end{bmatrix} \tag{49}$$

and is independent of the averaging scheme.

Now, we postulate that the optimal averaging scheme should be made up of $K = N - 3$ reduced-reflectometer calibrations that are least sensitive to measurement errors. We quantify this sensitivity with the quality factor (B.14) defined as the determinant of the error covariance matrix. Finding such an averaging scheme is a difficult combinatorial-optimization problem, related to the weighted set-cover problem [22]. However, obtaining the best solution of this problem is not necessary in our case. Indeed, as we noted earlier on, for averaging schemes that are constructed from well-conditioned reduced-reflectometer calibrations, we obtain approximately the same Fisher matrix (48). Thus, it is sufficient to find an averaging scheme that is close to the optimal one. An algorithm for finding such a scheme is described in Appendix C.

IV. Measurements

In this section, we present an experimental verification of our calibration method with on-wafer calibration standards. We first compare the propagation constant obtained from the multireflect-thru method and from a reference multiline TRL calibration. Following that, we apply the calibration comparison method [23] to compare the VNA calibration coefficients obtained with both methods. Finally, we evaluate results of corrected measurements of a mismatched line section, performed after calibrating VNA with our multireflect-thru method and with the reference multiline TRL method.

We implemented the calibration standards on a 500 μm thick quartz wafer (see Fig. 2). We used the coplanar waveguide (CPW) with 100 μm wide center strip, 10 μm gaps, and 240 μm wide ground strips. We implemented the multireflect-thru method with a set of eight offset shorts and a 420 μm long thru connection. Lengths of the offset shorts are (440, 1190, 1940, 2690, 3928, 6665, 10 790, and 17 390) μm. The lower frequency of this calibration was estimated to 3.4 GHz [19]. In the multiline TRL method, we used six lines, a 420 μm long thru connection, and a 920 μm long offset short as a reflect standard. Lengths of the lines are (1000, 3135, 4200, 7615, 12 570, and 17 298) μm. Measurements were performed with ZVA50 VNA in the frequency range 0.1–40 GHz, the IF bandwidth was set to 100 Hz. In order to avoid the microstrip-like mode, the quartz wafer was put on a 6 mm thick absorbing material.

In Fig. 3(a) and (b), we show the phase and attenuation constant obtained from reduced-reflectometer calibrations

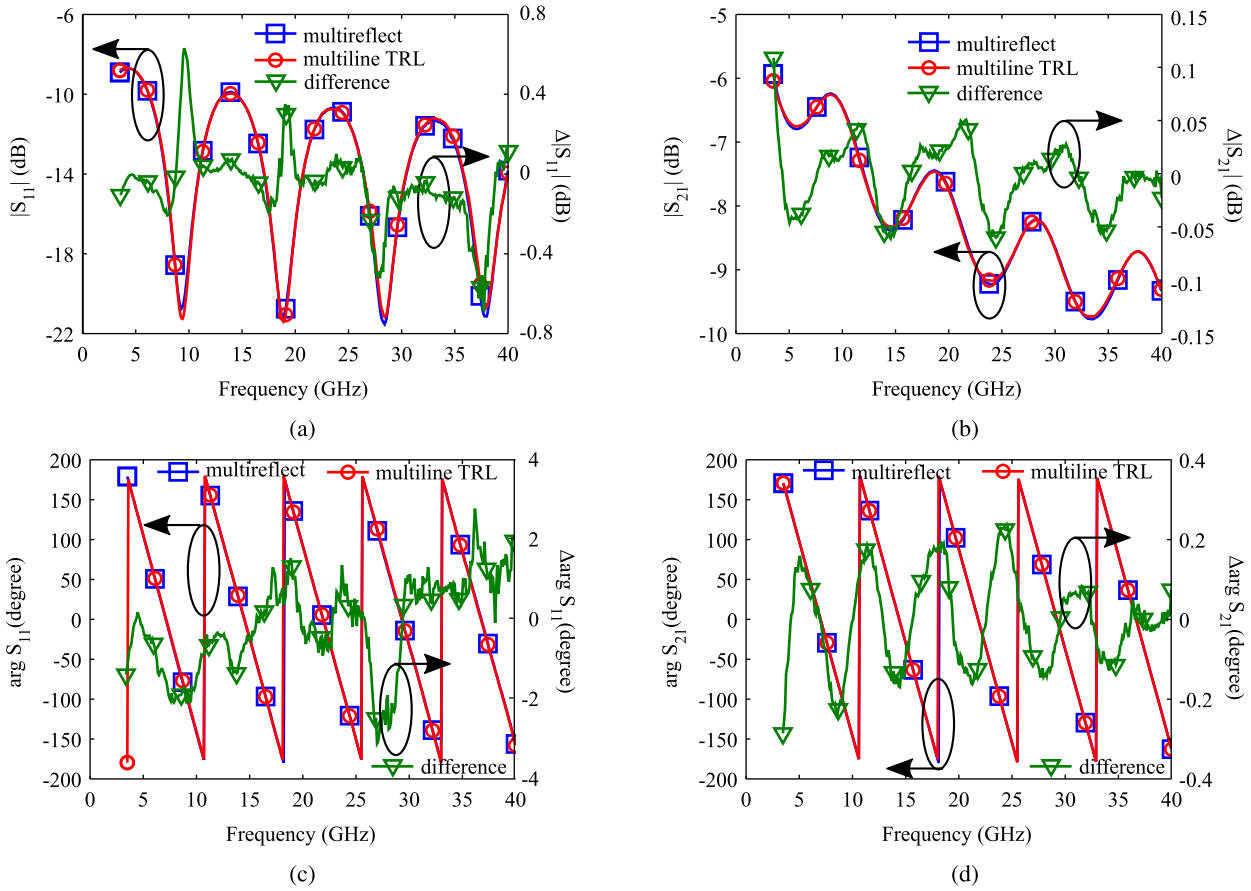

Fig. 5. Measurement of a mismatched line section obtained with the multireflect-thru calibration and with the reference multiline TRL method. (a), (b) Magnitude of S_{11} and S_{21}, respectively, obtained from the multireflect-thru calibration (blue solid line with squares) and the reference multiline TRL calibration (red solid line with circles) along with the difference (green solid line with triangles). (c), (d) Phase of S_{11} and S_{21}, respectively, obtained from the multireflect-thru calibration and from the reference multiline TRL calibration along with the difference (the same colors and markers as for the magnitude).

on each VNA port and from the reference multiline TRL calibration; we also show differences with respect to the multiline TRL results. We see that the results for both methods agree very well. Differences in the phase constant are smaller than 0.8°/cm and in the attenuation constant smaller than 0.13 dB/cm. We notice that these differences become larger as we approach the lower frequency of both calibrations, and thus both methods are more sensitive to measurement and modeling errors.

In Fig. 4, we compare the multireflect-thru and the reference multiline TRL calibration by use of the calibration comparison method [23]. In Fig. 4, we plot the estimates of worst case deviations due to nonrepeatability of the multireflect-thru and the reference multiline TRL calibrations (blue solid line with squares and red solid line with circles) and compare it with the estimate of worst case deviation due to the difference between the multireflect-thru and the reference multiline TRL calibration (green solid line with triangles). We observe that both calibration techniques have similar repeatability. We further see the worst case deviation due to the difference between these calibration techniques is comparable with the deviation due to the nonrepeatability. This error is at most 0.04 for frequencies above 4 GHz and increases to around 0.07 below 4 GHz where the multireflect-thru calibration is close to its lower frequency, and therefore more sensitive to measurement and modeling errors. Thus, since the method-to-method difference is on the same order as the inevitable repeatability errors, we conclude that both calibration techniques yield the same VNA calibration coefficients to an accuracy of repeatability errors.

In Fig. 5, we compare measurements of a mismatched line section obtained with the multireflect-thru and the reference multiline TRL calibrations. We see that the magnitudes of both S_{11} and S_{21} [see Fig. 5(a) and (b)] agree very well. The differences in $|S_{11}|$ are less than 0.2 dB (2.3%) apart from the regions with $|S_{11}| < 20$ dB where the differences increase to around 0.7 dB (8.4%). This can be explained by the fact that the multireflect-thru calibration uses primarily calibration standards with large reflection coefficients, hence its accuracy deteriorates for well-matched DUTs. The differences between the two calibrations for $|S_{21}|$ are less than 0.1 dB (1.2%) and increase at frequencies close to the lower frequency of the multireflect-thru calibration. We finally observe that the agreement between the two calibrations for phase of S_{11} and S_{21} [see Fig. 5(c) and (d)] is also very good with errors less than 2° for arg S_{11} and 0.3° for arg S_{21}. For the sake of comparison,

a probe placement error of ± 5 μm leads approximately to an error in $\arg S_{11}$ and $\arg S_{21}$ on the order of $\pm 0.8^\circ$ and $\pm 0.4^\circ$, respectively (assuming $\beta/\beta_0 = 1.7$ and $f = 40$ GHz).

V. Conclusion

We presented a new method for calibrating a two-port VNA with multiple offset reflects and a flush thru connection. Offset-reflect standards are constructed out of transmission-line sections with the same unknown propagation constant, and are terminated with the same unknown highly reflective load. The propagation constant of these sections and the load reflection coefficient are then determined simultaneously with the VNA calibration coefficients. In order to determine the propagation constant, our method requires to solve $N - 3$ independent complex-valued nonlinear equations where N is the number of offset reflects, while the remaining unknown parameters (i.e., VNA calibration coefficients and the load reflection coefficient) are calculated from closed-form expressions. This makes our method more robust than other similar approaches (see [7]–[9]) that may not yield a unique solution due to the use of optimization techniques. We verified our method experimentally by comparing on-wafer multireflect-thru and multiline TRL calibrations performed with CPW offset-reflects and transmission lines manufactured on a 500 μm thick quartz wafer. Both calibrations yielded similar values of the CPW propagation constant and of the VNA calibration coefficients confirming the validity of our calibration approach.

Our new multireflect-thru method, similar to the multiline TRL, uses calibration standards whose definitions require only dimensional measurement, thus it is possible to establish a traceability path for our approach to dimensional metrology. Thus, the multireflect-thru method constitutes an alternative to the multiline TRL calibration in environments in which the use of transmission lines is difficult, such as in the case VNAs with very small coaxial and waveguide connectors. Also, the multireflect-thru calibration, unlike the multiline TRL methods, allows for a design of on-wafer calibration substrates for which the distance between the probes is kept constant. Thus, it may be used to speed up and thus reduce the cost of large-scale automated testing in on-wafer environments.

Appendix A
Numerical Solution of (16)

We first note that through some algebraic manipulations, (16) can be expanded as

$$\begin{aligned}\det \mathbf{P}(\gamma) = {} & (\rho_0-\rho_1)(\rho_2-\rho_3)(\widetilde{\Gamma}_0-\widetilde{\Gamma}_3)(\widetilde{\Gamma}_2-\widetilde{\Gamma}_1)+ \\ & -(\rho_0-\rho_3)(\rho_2-\rho_1)(\widetilde{\Gamma}_0-\widetilde{\Gamma}_1)(\widetilde{\Gamma}_2-\widetilde{\Gamma}_3)=0\end{aligned} \tag{A.1}$$

which is equivalent to the condition

$$\frac{(\rho_0-\rho_1)(\rho_2-\rho_3)}{(\rho_0-\rho_3)(\rho_2-\rho_1)} = \frac{(\widetilde{\Gamma}_0-\widetilde{\Gamma}_1)(\widetilde{\Gamma}_2-\widetilde{\Gamma}_3)}{(\widetilde{\Gamma}_0-\widetilde{\Gamma}_3)(\widetilde{\Gamma}_2-\widetilde{\Gamma}_1)} \tag{A.2}$$

which is known as the condition for the cross-ratio invariance under the bilinear transformation. Now, in order to describe the algorithm for numerical solution of (A.1), we first write it in a more compact form

$$\begin{aligned}\det \mathbf{P}(\gamma) &\equiv f(\gamma) \\ &= A(\rho_0-\rho_1)(\rho_2-\rho_3) - B(\rho_0-\rho_3)(\rho_2-\rho_1) = 0\end{aligned} \tag{A.3}$$

where

$$A = (\widetilde{\Gamma}_0-\widetilde{\Gamma}_3)(\widetilde{\Gamma}_2-\widetilde{\Gamma}_1) \tag{A.4}$$

$$B = (\widetilde{\Gamma}_0-\widetilde{\Gamma}_1)(\widetilde{\Gamma}_2-\widetilde{\Gamma}_3). \tag{A.5}$$

In order to solve (A.3), we developed a modified Newton–Raphson method, which has improved robustness and convergence properties with respect to the classical Newton–Raphson method. In this modified method, we control the accuracy of the linear approximation such that the relative error of this approximation is smaller than some predefined value (in our case 5%). To this end, we write the first-order Taylor series expansion

$$f(\gamma_0+\Delta\gamma) \approx f(\gamma_0) + f'(\gamma_0)\Delta\gamma \tag{A.6}$$

where the first derivative is given by

$$\begin{aligned}f'(\gamma) = {} & 2A(l_0+l_3)\rho_0\rho_3 + 2A(l_1+l_2)\rho_1\rho_2 + \\ & -2B(l_0+l_1)\rho_0\rho_1 - 2B(l_2+l_3)\rho_2\rho_3 + \\ & +2(B-A)(l_0+l_2)\rho_0\rho_2 + 2(B-A)(l_1+l_3)\rho_1\rho_3.\end{aligned} \tag{A.7}$$

Then we proceed iteratively, where step in nth iteration is determined by

$$\Delta\gamma_n = -\delta\frac{f(\gamma_{n-1})}{f'(\gamma_{n-1})}\left|\frac{f'(\gamma_{n-1})}{f(\gamma_{n-1})}\right| \tag{A.8}$$

where the real factor $\delta = |\Delta\gamma_n|$ is the length of the step $\Delta\gamma_n$. We choose δ such that the error of the approximation (A.6) is less than 5%.

We estimate this error in the following manner. We write the expansion of the real and imaginary parts of $f(\gamma) = u(\gamma) + jv(\gamma)$ separately as

$$u(\gamma) = u(\gamma_0) + \mathrm{Re}\big[f'(\gamma_0)\Delta\gamma\big] + r_{u2}(\gamma) \tag{A.9}$$

$$v(\gamma) = v(\gamma_0) + \mathrm{Im}\big[f'(\gamma_0)\Delta\gamma\big] + r_{v2}(\gamma) \tag{A.10}$$

where $r_{u2}(\gamma)$ and $r_{v2}(\gamma)$ are the reminders of the Taylor's series. These reminders can be written as

$$r_{u2}(\gamma) = \frac{1}{2}\mathrm{Re}\big[f''(\xi_u)(\Delta\gamma)^2\big] \tag{A.11}$$

$$r_{v2}(\gamma) = \frac{1}{2}\mathrm{Im}\big[f''(\xi_v)(\Delta\gamma)^2\big] \tag{A.12}$$

and ξ_u and ξ_v are unknown complex numbers, and

$$\begin{aligned}f''(\gamma) = {} & -4A(l_0+l_3)^2\rho_0\rho_3 - 4A(l_1+l_2)^2\rho_1\rho_2 + \\ & +4B(l_0+l_1)^2\rho_0\rho_1 + 4B(l_2+l_3)^2\rho_2\rho_3 + \\ & -4(B-A)(l_0+l_2)^2\rho_0\rho_2 - 4(B-A)(l_1+l_3)^2\rho_1\rho_3.\end{aligned} \tag{A.13}$$

Now we can estimate the maximum value of r_{u2} as

$$|r_{u2}(\gamma)| = \frac{1}{4}\left|f''(\xi_u)(\Delta\gamma)^2 + f''(\xi_u)^*(\Delta\gamma^*)^2\right| \leq \leq \frac{1}{2}\left|f''(\xi_u)(\Delta\gamma)^2\right| = \frac{1}{2}\left|f''(\xi_u)\right||\Delta\gamma|^2 \leq \frac{1}{2}H|\Delta\gamma|^2 \tag{A.14}$$

where

$$H = \sup|f''(\xi_u)| = 4|A|(l_0+l_3)^2 + 4|A|(l_1+l_2)^2 + 4|B|(l_0+l_1)^2 + 4|B|(l_2+l_3)^2 + + 4|B-A|(l_0+l_2)^2 + 4|B-A|(l_1+l_3)^2.$$

In a similar manner, we can determine that also $|r_{u2}(\gamma)| \leq 1/2H|\Delta\gamma|^2$. Thus, the maximum error we make by the approximation (A.1) is

$$\Delta\epsilon = \left|f(\gamma_0+\Delta\gamma) - f(\gamma_0) - f'(\gamma_0)\Delta\gamma\right| \leq \sqrt{2\left(\frac{1}{2}H|\Delta\gamma|^2\right)^2} = \frac{H|\Delta\gamma|^2}{\sqrt{2}}. \tag{A.15}$$

Now if the relative error $\delta\epsilon = \Delta\epsilon/|f(\gamma)|$ should be less than some constant $\delta\epsilon_{\max}$, we have

$$\frac{\Delta\epsilon}{|f(\gamma)|} = \frac{H|\Delta\gamma|^2}{|f(\gamma)|\sqrt{2}} \leq \delta\epsilon_{\max} \tag{A.16}$$

so we obtain

$$\delta = |\Delta\gamma| \leq \sqrt{\delta\epsilon_{\max}\frac{\sqrt{2}|f(\gamma)|}{H}}. \tag{A.17}$$

APPENDIX B
ERROR ANALYSIS OF THE REDUCED-REFLECTOMETER CALIBRATION

In this appendix, we present an error analysis of the reduced-reflectometer calibration. Results of this analysis lay foundation for the calibration with a redundant number of offset-reflect standards (see Section III-B).

For a given set of measurements and definitions, we have a solution

$$\boldsymbol{\beta} = [E_1', E_2, E_3', \gamma]^T \tag{B.1}$$

of the reduced-reflectometer calibration problem (15). Let us assume that the calibration-standard reflection coefficients have relative errors

$$\Delta\mathbf{y} = \left[\frac{\Delta\rho_0}{\rho_0}, \frac{\Delta\rho_1}{\rho_1}, \frac{\Delta\rho_2}{\rho_2}, \frac{\Delta\rho_3}{\rho_3}\right]^T$$

which introduce a solution error

$$\Delta\boldsymbol{\beta} = [\Delta E_1', \Delta E_2, \Delta E_3', \Delta\gamma]^T. \tag{B.2}$$

We now want to find a relationship between errors $\Delta\mathbf{y}$ and $\Delta\boldsymbol{\beta}$. Assuming that errors are small, we can rewrite (15) to first order as

$$[\mathbf{P}(\gamma) + \Delta\mathbf{P}(\gamma, \Delta\gamma)](\mathbf{x}+\Delta\mathbf{x}) \approx \mathbf{P}(\gamma)\mathbf{x} + \Delta\mathbf{P}(\gamma, \Delta\gamma)\mathbf{x} + \mathbf{P}(\gamma)\Delta\mathbf{x} = \Delta\mathbf{P}(\gamma, \Delta\gamma)\mathbf{x} + \mathbf{P}(\gamma)\Delta\mathbf{x} = 0 \tag{B.3}$$

where

$$\Delta\mathbf{x} = [\Delta E_1', \Delta E_2, \Delta E_3', 0]^T. \tag{B.4}$$

Approximating matrix $\Delta\mathbf{P}(\gamma, \Delta\gamma)$ by use of the first order Taylor expansion $e^{-2(\gamma+\Delta\gamma)l} \approx e^{-2\gamma l}(1-2l\Delta\gamma)$, we further obtain

$$\Delta\mathbf{P}(\gamma, \Delta\gamma) \approx \begin{bmatrix} \Delta\rho_0 & 0 & \widetilde{\Gamma}_0\Delta\rho_0 & 0 \\ \Delta\rho_1 & 0 & \widetilde{\Gamma}_1\Delta\rho_1 & 0 \\ \Delta\rho_2 & 0 & \widetilde{\Gamma}_2\Delta\rho_2 & 0 \\ \Delta\rho_3 & 0 & \widetilde{\Gamma}_3\Delta\rho_3 & 0 \end{bmatrix} + - 2\Delta\gamma \begin{bmatrix} \rho_0 l_0 & 0 & \widetilde{\Gamma}_0\rho_0 l_0 & 0 \\ \rho_1 l_1 & 0 & \widetilde{\Gamma}_1\rho_1 l_1 & 0 \\ \rho_2 l_2 & 0 & \widetilde{\Gamma}_2\rho_2 l_2 & 0 \\ \rho_3 l_3 & 0 & \widetilde{\Gamma}_3\rho_3 l_3 & 0 \end{bmatrix}. \tag{B.5}$$

Inserting (B.5) into (B.3) leads after some straightforward manipulations to

$$\mathbf{X}\Delta\boldsymbol{\beta} = -\Delta\mathbf{y} \tag{B.6}$$

where

$$\mathbf{X} = \begin{bmatrix} \frac{1}{E_1+E_3\widetilde{\Gamma}_0} & \frac{\rho_0^{-1}}{E_1+E_3\widetilde{\Gamma}_0} & \frac{\widetilde{\Gamma}_0}{E_1+E_3\widetilde{\Gamma}_0} & -2l_0 \\ \frac{1}{E_1+E_3\widetilde{\Gamma}_1} & \frac{\rho_1^{-1}}{E_1+E_3\widetilde{\Gamma}_1} & \frac{\widetilde{\Gamma}_1}{E_1+E_3\widetilde{\Gamma}_1} & -2l_1 \\ \frac{1}{E_1+E_3\widetilde{\Gamma}_2} & \frac{\rho_2^{-1}}{E_1+E_3\widetilde{\Gamma}_2} & \frac{\widetilde{\Gamma}_2}{E_1+E_3\widetilde{\Gamma}_2} & -2l_2 \\ \frac{1}{E_1+E_3\widetilde{\Gamma}_3} & \frac{\rho_3^{-1}}{E_1+E_3\widetilde{\Gamma}_3} & \frac{\widetilde{\Gamma}_3}{E_1+E_3\widetilde{\Gamma}_3} & -2l_3 \end{bmatrix}. \tag{B.7}$$

Equation (B.6) relates the error $\Delta\boldsymbol{\beta}$ and $\Delta\mathbf{y}$ through the calibration coefficient E_1 and E_3, lengths l_i of the offset reflects, and their raw measurements $\widetilde{\Gamma}_i$, for $i = 0, \ldots, 3$. However, it would be more informative to express this relationship solely in terms of the reduced-reflectometer parameters and calibration-standard reflection coefficients. In order to obtain such a relationship, we eliminate $\widetilde{\Gamma}_i$ by inserting (10) into (B.7). We can show that this leads to the following equation:

$$\mathbf{X} = \mathbf{X}_0\mathbf{E} \tag{B.8}$$

where

$$\mathbf{X}_0 = \begin{bmatrix} \rho_0 & 1 & \rho_0^{-1} & -2l_0 \\ \rho_1 & 1 & \rho_1^{-1} & -2l_1 \\ \rho_2 & 1 & \rho_2^{-1} & -2l_2 \\ \rho_3 & 1 & \rho_3^{-1} & -2l_3 \end{bmatrix} \tag{B.9}$$

and

$$\mathbf{E} = \frac{1}{E_1'+E_2E_3'}\begin{bmatrix} -E_3' & 0 & E_1' & 0 \\ 1 & -E_3' & E_2 & 0 \\ 0 & 1 & 0 & 0 \\ 0 & 0 & 0 & E_1'+E_2E_3' \end{bmatrix}. \tag{B.10}$$

Equations (B.6) and (B.8) are our main result and are used in the averaging technique discussed in Section III-B. Based on these equations, we can also develop a quality factor for the reduced-reflectometer calibration which

is used in the algorithm for choosing the best set of reduced-reflectometer calibrations (i.e., the averaging scheme), discussed in Section III-C. We define this factor as the determinant of the covariance matrix of the solution (B.1) [17]. In order to calculate the covariance matrix of this vector, we assume that the most important error sources are connection nonrepeatability and errors in standard definitions, and we neglect the VNA raw measurement errors. We further assume that the real and imaginary parts of relative errors $\Delta\mathbf{y}$ have the same variance and are uncorrelated, while their mean value is zero. This is only an approximation, as in fact often one of the error components (typically the phase error) dominates. However, as demonstrated in [19], this approximation leads only to a slight overestimation of solution variances. Since the quality factor we develop will be used only to compare different reduced-reflectometer calibrations, we can accept this approximation.

Based on the above, the covariance matrix of $\Delta\mathbf{y}$ can be written with the use of complex notation as

$$\mathbf{\Sigma}_{\Delta\mathbf{y}} = \mathrm{E}[\Delta\mathbf{y}\Delta\mathbf{y}^H]. \tag{B.11}$$

Consequently, we can write

$$\mathbf{\Sigma}_{\Delta\boldsymbol{\beta}} = \mathrm{E}[\Delta\beta\Delta\beta^H] = \mathbf{E}^{-1}\mathbf{X}_0^{-1}\mathbf{\Sigma}_{\Delta\mathbf{y}}\mathbf{X}_0^{-H}\mathbf{E}^{-H}. \tag{B.12}$$

The determinant of this matrix can be now written as

$$\det\mathbf{\Sigma}_{\Delta\boldsymbol{\beta}} = \frac{|E_1' + E_2E_3'|^4 \det\mathbf{\Sigma}_{\Delta\mathbf{y}}}{\det(\mathbf{X}_0^H\mathbf{X}_0)}. \tag{B.13}$$

We see that this determinant depends on calibration standard parameters, the covariance matrix of errors, and the reduced-reflectometer parameters. Since the dependence on the reduced-reflectometer parameters is by a constant multiplication factor, we can introduce the normalized determinant of the covariance matrix

$$q = \frac{\det\mathbf{\Sigma}_{\Delta\boldsymbol{\beta}}}{|E_1' + E_2E_3'|^4} = \frac{\det\mathbf{\Sigma}_{\Delta\mathbf{y}}}{\det\mathbf{X}_0^H\mathbf{X}_0} \tag{B.14}$$

which will be our quality factor. We finally observe that the smaller is the quality factor q, the smaller are calibration errors.

APPENDIX C
APPROXIMATE ALGORITHM FOR FINDING THE AVERAGING SCHEME

We first analyze all of the C_4^N subsets to find the one with the best quality factor (B.14). Let this first subset contain offset reflects with indices $\mathbf{i}_0 = [i_{0_0}, i_{0_1}, i_{0_2}, i_{0_3}]^T$. Let us further define the set ϕ that contains indices of reflects that have already been included in the averaging scheme. After choosing the first four-element subset $\mathbf{i}_0$, we have $\phi_0 = \{i_{0_0}, i_{0_1}, i_{0_2}, i_{0_3}\}$.

Now, when constructing the kth subset we look for the best four-element subset according to the quality factor (B.14), whose three elements belong to the set ϕ_{k-1} while the fourth element to the set $\{0, \ldots, N-1\} \setminus \phi_{k-1}$. Let this subset have indices $\mathbf{i}_k = [i_{k_0}, i_{k_1}, i_{k_2}, i_{k_3}]^T$, where $i_{k_0}, i_{k_1}, i_{k_2} \in \phi_{k-1}$ and $i_{k_3} \in \{0, \ldots, N-1\} \setminus \phi_{k-1}$. We then update $\phi_k = \phi_{k-1} \cup i_{k_3}$ and proceed to the choice of the $(k+1)$th subset until all of the reflects have been added to the averaging scheme.

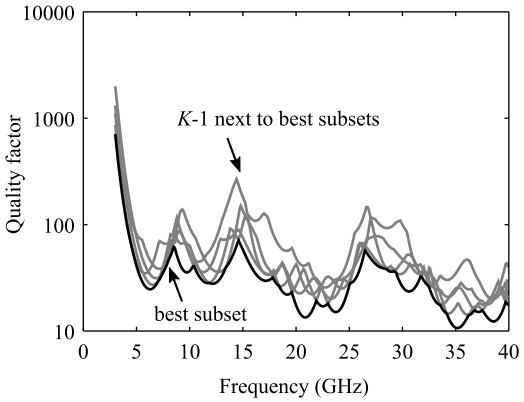

Fig. 6. Quality factor (B.14) for K best subsets calculated for eight quartz-CPW offset shorts discussed in Section IV.

In Fig. 6, we show results of this algorithm for eight CPW offset shorts used to implement the multireflect-thru considered in Section IV. We show there the quality factor (B.14) for K best subsets computed independently at each frequency. We observe that (B.14) for all of the subsets is frequency dependent and increases close to the lower frequency of the calibration where the phase shifts off all offset shorts become comparable.

REFERENCES

[1] I. Kasa, "Closed-form mathematical solutions to some network analyzer calibration equations," *IEEE Trans. Instrum. Meas.*, vol. IM-23, no. 4, pp. 399–402, Dec. 1974.

[2] B. Bianco and M. Parodi, "Measurement of the effective relative permittivities of microstrip," *Electron. Lett.*, vol. 11, no. 3, pp. 71–72, Feb. 1975.

[3] G. F. Engen, "Calibration technique for automated network analyzers with application to adapter evaluation," *IEEE Trans. Microw. Theory Techn.*, vol. MTT-22, no. 12, pp. 1255–1259, Dec. 1974.

[4] G. F. Engen, "Calibrating the six-port reflectometer by means of sliding terminations," *IEEE Trans. Microw. Theory Techn.*, vol. MTT-26, no. 12, pp. 951–957, Dec. 1978.

[5] W. Wiatr, "A method for embedding network characterization with application to low-loss measurements," *IEEE Trans. Instrum. Meas.*, vol. IM-36, no. 2, pp. 487–490, Jun. 1987.

[6] W. Sigg and J. Simon, "Reflectometer calibration using load, short and offset shorts with unknown phase," *Electron. Lett.*, vol. 27, no. 18, pp. 1650–1651, Aug. 1991.

[7] W. Wiatr and A. Lewandowski, "Multiple reflect technique for wideband one-port VNA calibration," in *Proc. 16th Int. Conf. Microw., Radar, Wireless Commun. (MIKON)*, Kraków, Poland, May 2006, pp. 37–40.

[8] J. Hoffmann, P. Leuchtmann, and R. Vahldieck, "Over-determined offset short calibration of a VNA," in *IEEE MTT-S Int. Microw. Symp. Dig.*, Atlanta, GA, USA, Jun. 2008, pp. 47–50.

[9] W. Wiatr, "Statistical VNA calibration technique using thru and multiple reflect terminations," in *Proc. 17th Int. Conf. Microw., Radar Wireless Commun.*, May 2008, pp. 1–2.

[10] R. B. Marks, "A multiline method of network analyzer calibration," *IEEE Trans. Microw. Theory Techn.*, vol. 39, no. 7, pp. 1205–1215, Jul. 1991.

[11] R. B. Marks, "Formulations of the basic vector network analyzer error model including switch-terms," in *50th ARFTG Conf. Dig.*, Portland, OR, USA, Dec. 1997, pp. 115–126.

[12] W. H. Press, S. A. Teukolsky, W. T. Vetterling, and B. P. Flannery, *Numerical Recipes 3rd Edition: The Art of Scientific Computing*, 3rd ed. New York, NY, USA: Cambridge Univ., 2007.

[13] B. Bianco, M. Parodi, S. Ridella, and F. Selvaggi, "Launcher and microstrip characterization," *IEEE Trans. Instrum. Meas.*, vol. IM-25, no. 4, pp. 320–323, Dec. 1976.
[14] G. F. Engen and C. A. Hoer, "Thru-reflect-line: An improved technique for calibrating the dual six-port automatic network analyzer," *IEEE Trans. Microw. Theory Techn.*, vol. MTT-27, no. 12, pp. 987–993, Dec. 1979.
[15] L. Mirsky, *An Introduction to Linear Algebra*. Oxford, U.K.: Clarendon, 1961.
[16] D. F. Williams, C.-F. Wang, and U. Arz, "In-phase/quadrature covariance-matrix representation of the uncertainty of vectors and complex numbers," in *Proc. 68th ARFTG Microw. Meas. Conf.*, Broomfield, CO, USA, Nov. 2006, pp. 62–65.
[17] R. Deutsch, *Estimation Theory*. Upper Saddle River, NJ, USA: Prentice-Hall, 1965.
[18] J. Groß, "The general Gauss-Markov model with possibly singular dispersion matrix," *Statist. Papers*, vol. 45, pp. 311–336, Jul. 2004.
[19] A. Lewandowski, W. Wiatr, L. J. Opalski, and R. Biedrzycki, "Accuracy and bandwidth optimization of the over-determined offset-short reflectometer calibration," *IEEE Trans. Microw. Theory Techn.*, vol. 63, no. 3, pp. 1076–1089, Mar. 2015.
[20] B. D. Hall, "On the propagation of uncertainty in complex-valued quantities," *Metrologia*, vol. 41, no. 3, p. 173, Apr. 2004.
[21] C. R. Rao and S. K. Mitra, "Generalized inverse of a matrix and its applications," in *Proc. 6th Berkeley Symp. Math. Statist. Probab.*, vol. 1. 1972, pp. 601–620.
[22] B. Korte and J. Vygen, *Combinatorial Optimization: Theory and Algorithms*. Berlin, Germany: Springer, 2012.
[23] D. F. Williams, R. B. Marks, and A. Davidson, "Comparison of on-wafer calibrations," in *38th ARFTG Conf. Dig.*, vol. 20. Dec. 1991, pp. 68–81.

Arkadiusz Lewandowski (M'09) received the M.Sc. and Ph.D. (Hons.) degrees in electrical engineering from the Warsaw University of Technology, Warsaw, Poland, in 2001 and 2010, respectively.

He joined the Institute of Electronics Systems, Warsaw University of Technology, in 2002, where he conducted research in the area of microwave measurements. From 2002 to 2004, he was with the Telecommunications Research Institute, Warsaw, where he was involved in the development of digital synthesizers of radar signals. From 2004 to 2008, he was a Guest Researcher with the National Institute of Standards and Technology, Boulder, CO, USA, where he was involved in the development of uncertainty analysis and calibration methods for coaxial and on-wafer VNA measurements. He has authored or co-authored over 50 scientific papers. His current research interests include small- and large-signal microwave measurements, and modeling of passive and active microwave devices.

Dr. Lewandowski was a recipient of the 2010 Warsaw University of Technology Award for Scientific Achievements, the Best Paper Award at the International Microwave Conference MIKON 2008, Poland, and the 2005 IEEE Microwave Theory and Techniques Society (MTT-S) Graduate Fellowship Award.

Wojciech Wiatr (M'96) received the M.Sc. and Ph.D. degrees in electronics engineering from the Warsaw University of Technology, Warsaw, Poland, in 1970 and 1980, respectively.

Since 1972, he has been with the Institute of Electronic Systems, Warsaw University of Technology, where he is currently an Assistant Professor. He has been developing new techniques and instrumentation for broadband scattering and noise parameter measurements of microwave transistors and monolithic microwave integrated circuits. He is an inventor of the RF multistate total power radiometer realizing simultaneous noise and vector analysis of microwave networks with natural noise excitation. In noise metrology, he collaborated with the National Radio Astronomy Observatory at Charlottesville, VA, USA, and the Ferdinand-Braun-Institut für Höchstfrequenztechnik, Berlin, Germany, and the National Institute of Standards and Technology, Boulder, CO, USA. He has authored one book, over 90 papers, and holds two patents. His current research interests include precision microwave measurements.

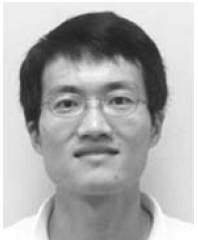

Dazhen Gu (SM'10) received the Ph.D. degree in electrical engineering from the University of Massachusetts, Amherst, MA, USA, in 2007. His doctoral research focused on the development of terahertz imaging components and systems.

He has been with the Electromagnetics Division, National Institute of Standards and Technology, Boulder, CO, USA, since 2003. In 2007, he joined the Microwave Measurement Services project, where he has been involved in microwave metrology, in particular thermal noise measurements and instrumentation. His current research interests include microfabrication, RF nanowire metrology, and calibration techniques for remote sensing.

Nathan D. Orloff was born in Columbia, SC, USA, in 1981. He received the B.S. (Hons.) and Ph.D. degrees in physics from the University of Maryland, College Park, MD, USA, in 2004 and 2010, respectively. His doctoral thesis involved the study and extraction of microwave properties of Ruddlesden-Popper ferroelectrics.

In 2011, he was a Dean's Post-Doctoral Fellow with Prof. I. R-. Kruse at the Department of Bioengineering, Stanford University, Stanford, CA, USA. He joined the Materials Measurement Laboratory, National Institute of Standards and Technology, Gaithersburg, MD, USA, in 2013, as a Rice University Post-Doctoral Fellow with Prof. M. Pasquali and joined the Communications Technology to lead the effort in microwave materials metrology in 2014.

Dr. Orloff was a recipient of the 2004 Martin Monroe Undergraduate Research Award, the 2006 CMPS Award for Excellence as a Teaching Assistant, the 2010 Michael J. Pelczar Award for Excellence in Graduate Study, and the 2015 Communications Laboratory Distinguished Associate Award.

James Booth, photograph and biography not available at the time of publication.